Local Integral Equations and two Meshless Polynomial Interpolations with Application to Potential Problems in Non-homogeneous Media

V. Sladek[1], J. Sladek[1], and M. Tanaka[2]

Abstract: An efficient numerical method is proposed for 2-d potential problems in anisotropic media with continuously variable material coefficients. The method is based on the local integral equations (utilizing a fundamental solution) and meshfree approximation of field variable. A lot of numerical experiments are carried out in order to study the numerical stability, accuracy, convergence and efficiency of several approaches utilizing various interpolations.

keyword: Integral equations, fundamental solution, subdomain, continuous non-homogeneity, anisotropy

1 Introduction

In the past years, the functionally graded materials (FGMs) are widely studied because of their excellent properties [Miyamoto et al (1999)]. The phenomenological description of such modern engineering materials within continuum theories is characterized by position dependent material coefficients. Moreover, owing to the composite structure the material properties are directionally dependent or anisotropic too. Hence, it follows the demand on the development of efficient numerical methods and subsequently the computer codes incorporating the spatial variations of material coefficients. Although the versatile and well established finite element method (FEM) and the boundary integral equation method (BIEM) or boundary element method (BEM) are basically applicable to such problems, some difficulties may occur in the numerical analysis. The material coefficients in commercial FEM codes are usually assumed to be constant within each domain cell, while the advantages of the integral equation formulations can be exploited only when the fundamental solution of the governing differential operator is available.

Recently, an increasing attention has been devoted to the extension of the applicability of integral equations based formulations to the solution of boundary value problems (BVPs) when the proper fundamental solution is not available in a simple form with aiming to get a formulation resulting in sparse system matrix like in FEM. One of such proposals concerns the utilization of the local integral equations (LIE) or a combination of the global and the local integral equations with implementing them either by the standard finite-size discretization elements or the moving least squares (MLS) approximation [Sladek, V. et al (2000), (2002), (2003), (2004), Sladek, J. et al (2002), (2004a), (2004b)]. Mikhailov (2002) and Mikhailov and Nakhova (2003) proposed to use localized boundary-domain integral equations to the solution of BVPs governed by PDEs with variable coefficients. The fundamental solution is replaced by a parametrix (Levi function) in their formulations.

In the last decade, great attention is also paid to various meshfree approximations in combination with both the variational and the integral equation formulations. The motivation consists in the main goal to avoid difficulties associated with the mesh generation especially in 3-D problems, and remeshing for moving BVPs such as fast crack propagation in fracture mechanics. The Meshless Petrov-Galerkin (MLPG) method by Atluri and Zhu (1998a, 1998b, 1999) proposed a family of new integration methods based on a local weak formulation [Atluri and Shen (2002a), (2002b), Atluri (2004)]. According to the choice of the test and trial functions, the MLPG results into various meshless formulations including the LBIE formulation [Zhu, Zhang & Atluri (1998), Sladek, J. et al (2002), Li et al (2003)]. These methods are expected to replace the mesh-based finite-element and boundary-element methods that are the basis of the current computational-software. The monograph [Atluri (2004)] presents, in a very self-contained fashion, the de-

[1] Institute of Construction and Architecture, Slovak Academy of Sciences, 845 03 Bratislava, Slovak Republic e-mail: *Vladimir.Sladek@savba.sk*; *Jan.Sladek@savba.sk*
[2] Department of Mechanical Systems Engineering, Shinshu University, 4-17-1 Wakasato, Nagano, 380-8553, Japan

tails of the methodology as well as numerical implementation of meshless methods.

In this paper, we present a new formulation for numerical solution of 2-D potential problems in continuously nonhomogeneous media. Isolated knots are spread over the whole analyzed domain including its boundary and each knot is surrounded virtually by a small subdomain of a simple geometrical form. The field variables are approximated by using meshfree Point Interpolation Methods (PIM) utilizing the polynomial basis functions as well as the radial basis functions [Liu (2003)]. The prescribed boundary conditions are collocated at boundary knots while at interior knots we consider the local integral equations as coupling relationships among the potential values at knots. The integral equations are nonsingular, the system matrix is sparse like in finite element method formulations and the method is sufficiently simple and quite general. A lot of numerical experiments has been carried out in order to test: 1) the numerical stability with respect to certain free parameters of the formulation as well as to distribution of knots; 2) the accuracy; 3) convergence of numerical results with increasing the density of knots, and finally to compare the CPU-times consumed by various numerical implementations including also the polynomial interpolation within standard discretization elements.

2 Local integral equation formulation for solution of boundary value problems

The potential problem (e.g. stationary heat conduction) in anisotropic and continuously non-homogeneous media is governed by the following partial differential equation with variable coefficients [Wrobel (2002)]

$$(\lambda_{ik}(\mathbf{x})u_{,k}(\mathbf{x}))_{,i} = -Q(\mathbf{x}), \text{in } \Omega \tag{1}$$

where $u(\mathbf{x})$ is the unknown potential field, $Q(\mathbf{x})$ is the known body source density, and $\lambda_{ik}(\mathbf{x})$ describe the spatial variation of the material coefficients related to the flux vector $q_i(\mathbf{x})$ as

$$q_i(\mathbf{x}) = -\lambda_{ik}(\mathbf{x})u_{,k}(\mathbf{x}) \quad . \tag{2}$$

Physically, Eq. (2) is known as the Fourier law for heat conduction or also as the first Fick's law in diffusion problems.

The prescribed boundary conditions (b.c.) can be classified as

(i) Dirichlet b.c.: $u(\eta) = \overline{u}(\eta)$ at $\eta \in \partial\Omega_D$

(ii) Neumann b.c.: $n_i(\eta)q_i(\eta) = \overline{q}(\eta)$ at $\eta \in \partial\Omega_N$

(iii) Robin b.c.: $\alpha u(\eta) + \beta n_i(\eta)q_i(\eta) = 0$ at $\eta \in \partial\Omega_R$, $(\alpha, \beta \in R)$

where $\partial\Omega = \partial\Omega_D \cup \partial\Omega_N \cup \partial\Omega_R$, $n_i(\eta)$ is the unit outward normal vector to the boundary, and an over bar denotes the prescribed quantities.

The use of methods based on integral equations utilizing fundamental solutions is approved because of the existence and the uniqueness of the solution of BVPs. It is well known that a pure boundary formulation is applicable to solution of the above mentioned boundary value problems only if the fundamental solution for the governing differential operator is available. Otherwise, the degrees of freedom (DOF) on the boundary as well as inside the analyzed domain are to be employed in the numerical solution. Owing to the lack of the fundamental solution for the differential operator with variable coefficients, it is appropriate to rewrite Eq. (1) as

$$\lambda_{ij}^c u_{,ij}(\mathbf{x}) + \left(\tilde{\lambda}_{ij}(\mathbf{x})u_{,j}(\mathbf{x})\right)_{,i} = -Q(\mathbf{x}) \quad , \tag{3}$$

where $\lambda_{ij}^c = \lambda_{ij}(\mathbf{x}^c)$, and $\tilde{\lambda}_{ij}(\mathbf{x}) = \lambda_{ij}(\mathbf{x}) - \lambda_{ij}^c$ is a fluctuation of the material coefficients inside a sub-domain Ω^c surrounding the point $\mathbf{x}^c$.

Let $G(\mathbf{x} - \mathbf{y})$ be the fundamental solution of the governing equation with constant coefficients in an infinite space

$$\lambda_{ij}^c G_{,ij}(\mathbf{x} - \mathbf{y}) = -\delta(\mathbf{x} - \mathbf{y}) \quad . \tag{4}$$

According to Chang et al. (1973), we may write in 2-d case

$$G(\mathbf{x} - \mathbf{y}) = -\frac{1}{2\pi\sqrt{|\Lambda^c|}}\ln\left(\sqrt{R}\right), R = (\lambda^c)_{ij}^{-1} r_i r_j$$

$$r_i = x_i - y_i \tag{5}$$

where $|\Lambda^c|$ denotes the determinant of the matrix $\mathbf{\Lambda}^c$ whose matrix elements are given by λ_{ij}^c. Starting from the integral identity

$$\int\limits_{\Omega^c} G(\mathbf{x} - \mathbf{y}^c)(\lambda_{ij}(\mathbf{x})u_{,j}(\mathbf{x}))_{,i} d\Omega(\mathbf{x}) =$$

$$-\int\limits_{\Omega^c} G(\mathbf{x} - \mathbf{y}^c)Q(\mathbf{x})d\Omega(\mathbf{x}) \tag{6}$$

and making use of the Gauss divergence theorem, we arrive at the integral relationship

$$
\int\limits_{\partial\Omega^c} \lambda_{ij}(\eta)u_{,j}(\eta)n_i(\eta)G(\eta-\mathbf{y}^c)\mathrm{d}\Gamma(\eta) -
$$
$$
\int\limits_{\Omega^c} \lambda_{ij}(\mathbf{x})u_{,j}(\mathbf{x})G_{,i}(\mathbf{x}-\mathbf{y}^c)\mathrm{d}\Omega(\mathbf{x}) =
$$
$$
-\int\limits_{\Omega^c} Q(\mathbf{x})G(\mathbf{x}-\mathbf{y}^c)\mathrm{d}\Omega(\mathbf{x}) \tag{7}
$$

in which $\mathbf{y}^c \in \Omega^c$. This integral equation can be used as a coupling equation for the evaluation of the unknown nodal values when a domain-type approximation is employed for the field variable. It will be referred to as the LIE (Local Integral Equation) of the 1st kind. Strictly speaking, Eq. (7) is an integro-differential equation for the unknown potential field.

Splitting λ_{ij} as $\lambda_{ij} = \lambda_{ij}^c + \tilde{\lambda}_{ij}$ in the second integral term of Eq. (7), applying the Gauss divergence theorem to the term involving λ_{ij}^c, and invoking of Eq. (4), we may write

$$
\int\limits_{\Omega^c} \lambda_{ij}(\mathbf{x})u_{,j}(\mathbf{x})G_{,i}(\mathbf{x}-\mathbf{y}^c)\mathrm{d}\Omega(\mathbf{x}) =
$$
$$
\int\limits_{\Omega^c} \tilde{\lambda}_{ij}(\mathbf{x})u_{,j}(\mathbf{x})G_{,i}(\mathbf{x}-\mathbf{y}^c)\mathrm{d}\Omega(\mathbf{x}) +
$$
$$
\int\limits_{\partial\Omega^c} u(\eta)\lambda_{ij}^c n_j(\eta)G_{,i}(\eta-\mathbf{y}^c)\mathrm{d}\Gamma(\eta) + u(\mathbf{y}^c) . \tag{8}
$$

Eventually, from Eqs. (7) and (8) we obtain the LIE of the 2nd kind

$$
u(\mathbf{y}^c) = \int\limits_{\partial\Omega^c} [\lambda_{ij}(\eta)u_{,j}(\eta)n_i(\eta)G(\eta-\mathbf{y}^c) -
$$
$$
u(\eta)\lambda_{ij}^c n_j(\eta)G_{,i}(\eta-\mathbf{y}^c)\big] \, d\Gamma(\eta) +
$$
$$
\int\limits_{\Omega^c} \Big[Q(\mathbf{x})G(\mathbf{x}-\mathbf{y}^c) - \tilde{\lambda}_{ij}(\mathbf{x})u_{,j}(\mathbf{x})G_{,i}(\mathbf{x}-\mathbf{y}^c)\Big]d\Omega(\mathbf{x}).
$$
$$
\tag{9}
$$

Note here that Eq. (9) is the integral representation of the potential at an interior point $\mathbf{y}^c$ in terms of the boundary densities of the potential $u(\eta)$ and the flux $q(\eta)$ as well as the gradients of the potential field in the interior of the sub-domain $\Omega^c \subset \Omega$. Some of the boundary densities can be prescribed by boundary conditions

when $\partial\Omega^c \cap \partial\Omega \neq \emptyset$. Contrary to the pure boundary integral representation, the dimensionality of the problem governed by (7) or (9) is not reduced because of the unknown potential gradients in the domain.

3 Meshless polynomial basis interpolations

The aim is to create shape functions for approximation of the field variable $u(\mathbf{x})$ within a subdomain using only nodes scattered arbitrarily in the analyzed domain without any predefined mesh to provide connectivity of the nodes. Assuming a finite series representation of the potential field in a subdomain Ω^q surrounding the nodal point $\mathbf{x}^q$, we have the approximated field given as

$$
u(\mathbf{x})|_{\Omega^q} = \sum_{a=1}^{N} B^a(\mathbf{x})c^a(\mathbf{x}^q) \tag{10}
$$

where $B^a(\mathbf{x})$ are the basis functions defined in the Cartesian coordinate space, N is the number of nodes in the support domain of the point $\mathbf{x}^q$, and $c^a(\mathbf{x}^q)$ are the expansion coefficients corresponding to the given point $\mathbf{x}^q$. Such an approximation belongs to Point Interpolation Methods (PIM) [Liu (2003)]. Selecting the basis functions as monomials or radial functions, one obtains the Polynomial PIM or Radial PIM, respectively. The Polynomial PIM exhibits excellent properties (consistency, shape functions possess the Kronecker delta properties) as long as the moment matrix is invertible [Liu (2003)]. Unfortunately, the singularity of the moment matrix is dependent on the nodal points distribution. There are proposed several techniques to avoid singular moment matrix [Liu (2003)]. On the other hand, in the case of Radial PIM the moment matrix is nonsingular but the consistency is not guaranteed and the accuracy of the approximation is sensitive with respect to the choice of shape parameters.

One of the ways how to ensure the reproduction of the linear field (C^1 consistency) in Radial PIM as well as to avoid singularity of the moment matrix in the Polynomial PIM is to use Radial-Polynomial basis [Liu (2003)]. Usually, the number of nodes N is determined by the number of the nodes in the support domain. In this paper, we predefine the number N and the supporting nodes are specified as N the nearest nodal points to the given point $\mathbf{x}^q$. Two different kinds of the modification of the polynomial basis by multiquadrics are employed in order to avoid the singularity of the moment matrix and to

stabilize the accuracy on the properly selected shape parameter involved in the multiquadrics.

3.1 *PBF×MQ interpolation approach*

Let $n(q,k)$ be the global number of the k-th nearest nodal point of N supporting nodes corresponding to $\mathbf{x}^q$. Thus, $n(q,1) = q$ and $\left|\mathbf{x}^{n(q,k)} - \mathbf{x}^q\right| \leq \left|\mathbf{x}^{n(q,k+1)} - \mathbf{x}^q\right|$ for $k = 2, ..., N$. Taking the basis functions in Eq. (10) as $B^n(\mathbf{x}) = P^k(\mathbf{x})R^{n(q,k)}(\mathbf{x})$, we can write

$$u(\mathbf{x})|_{\Omega^q} = \sum_{k=1}^{N} P^k(\mathbf{x})R^{n(q,k)}(\mathbf{x})c^{(q,k)}, \tag{11}$$

where the polynomial basis is given by monomials $P^k(\mathbf{x}) \in \left\{1, x_1, x_2, x_1x_2, x_1^2, x_2^2\right\}$ for $k = 1, ..., (N = 6)$ and the radial basis is given by multiquadrics [Hardy (1990)]

$$R^n(\mathbf{x}) = \left(|\mathbf{x} - \mathbf{x}^n|^2 + c^2\right)^{m/2},$$

with c and m being the shape parameters. Usually, it is appropriate to select a dimensionless shape parameter γ by $c = \gamma h$, where h is the characteristic length defined as the shortest distance of any two nodal points distributed over the closed domain $\Omega \cup \partial\Omega$. The choice $N = 6$ is corresponding to the use of complete quadratic polynomial basis.

The expansion coefficients $c^{(q,k)}$ can be determined by enforcing that Eq. (11) be satisfied at N supporting nodes corresponding to $\mathbf{x}^q$. Thus, we have a system of N equations

$$\sum_{k=1}^{N} M^{jk}c^{(q,k)} = u(\mathbf{x}^{n(q,j)}) \quad , \quad (j = 1, ..., N)$$

in which $M^{jk} := P^k(\mathbf{x}^{n(q,j)})R^{n(q,k)}(\mathbf{x}^{n(q,j)})$. Hence, and from Eq. (11), the potential field is approximated in terms of its nodal values and the shape functions corresponding to supporting nodes as

$$u(\mathbf{x})|_{\Omega^q} = \sum_{j=1}^{N} u(\mathbf{x}^{n(q,j)})\varphi^{(q,j)}(\mathbf{x}) \quad , \tag{12}$$

where the shape function is given by

$$\varphi^{(q,j)}(\mathbf{x}) = \sum_{k=1}^{N} P^k(\mathbf{x})R^{n(q,k)}(\mathbf{x})\left(M^{-1}\right)^{kj} \quad . \tag{13}$$

Note that the matrix M^{jk} is not given by the product of matrices $P^{jl} = P^l\left(\mathbf{x}^{n(q,j)}\right)$ and $R^{lk} = R^{n(q,k)}\left(\mathbf{x}^{n(q,l)}\right)$. Hence, the possible singularity of the matrix P^{jl} does not yield singularity of the matrix M^{jk}. Moreover, the invertibility of the matrix R^{jk} [Liu (2003)] gives rise to anticipation of the invertibility of the matrix M^{jk}.

The shape and size of the subdomain Ω^q can be chosen arbitrarily. In numerical calculations, we have considered circular subdomains of radius h.

The gradients of the potential field are approximated as

$$u_{,i}(\mathbf{x})|_{\Omega^q} = \sum_{j=1}^{N} u(\mathbf{x}^{n(q,j)})\varphi_{,i}^{(q,j)}(\mathbf{x}) \tag{14}$$

where

$$\varphi_{,i}^{(q,j)}(\mathbf{x}) =$$

$$\sum_{k=1}^{N} \left[P_{,i}^k(\mathbf{x})R^{n(q,k)}(\mathbf{x}) + P^k(\mathbf{x})R_{,i}^{n(q,k)}(\mathbf{x})\right]\left(M^{-1}\right)^{kj}$$

$$P_{,i}^k(\mathbf{x}) \in \left\{0, \delta_{i1}, \delta_{i2}, x_2\delta_{i1} + x_1\delta_{i2}, 2x_1\delta_{i1}, 2x_2\delta_{i2}\right\},$$

if $N = 6$

$$R_{,i}^n(\mathbf{x}) = m\frac{x_i - x_i^n}{\left(|\mathbf{x} - \mathbf{x}^n|^2 + c^2\right)^{1-m/2}}$$

Apparently, $\varphi^{(q,j)}(\mathbf{x}^{n(q,l)}) = \delta_{jl}$, i.e. the shape functions possess the Kronecker delta property and the potential field is expressed according to (12) in terms of its nodal values.

3.2 *PBF+MQ and PBF interpolation approaches*

In this approach, the field variable is approximated as

$$u(\mathbf{x})|_{\Omega^q} = \sum_{k=1}^{N} R^{n(q,k)}(\mathbf{x})\alpha^{(q,k)} + \sum_{k=1}^{M} P^k(\mathbf{x})\beta^{(q,k)}, \tag{15}$$

where N is again the number of supporting nodes while M can be different from N, in general. Liu (2003) selects M on the reproduction requirement and advices to use $M < N$ for better stability. Let us consider $M \leq N$ with M corresponding to the number of monomials for a complete polynomial interpolation with selected order.

Collocating Eq. (15) at supporting nodes, one can get the system of equations

$$\sum_{k=1}^{N} R^{jk}\alpha^{(q,k)} + \sum_{k=1}^{M} P^{jk}\beta^{(q,k)} = u(\mathbf{x}^{n(q,j)})$$
$$(j = 1, ..., N),$$

(16)

where $R^{jk} = R^{n(q,k)}\left(\mathbf{x}^{n(q,j)}\right)$ and $P^{jk} = P^k\left(\mathbf{x}^{n(q,j)}\right)$. In order to determine the expansion coefficients in (15) uniquely, extra constraint equations are required [Liu (2003), Golberg et al (1999)]. It will be seen that the choice of the constraint equation as

$$\sum_{k=1}^{N} \alpha^{(q,k)} P^{kj} = 0 , \quad (j = 1, ..., M)$$

(17)

yields the Kronecker delta property for the resulting shape function.

In order to express the expansion coefficients in terms of the nodal values of the field variable, we shall assume q to be fixed and the summation rule over the repeated superscripts. Thus, Eqs. (16) and (17) can be written briefly as

$$R^{jk}\alpha^k + P^{jk}\beta^k = u^j , \quad (j = 1, ..., N)$$

(16*)

$$\alpha^k P^{kj} = 0 , \quad (j = 1, ..., M).$$

(17*)

In view of Eq. (16*), we have

$$\alpha^k = (R^{-1})^{kj}\left(u^j - P^{jl}\beta^l\right)$$

(18)

hence and from (17*),

$$\beta^l = Q^{lj}u^j,$$

(19)

where

$$Q^{lj} := (S^{-1})^{lm}(P^T)^{mk}(R^{-1})^{kj},$$
$$S^{ml} := (P^T)^{mk}(R^{-1})^{kj}P^{jl} \quad .$$

Finally, from (18) and (19), we obtain

$$\alpha^k = T^{kj}u^j, \quad T^{kj} := (R^{-1})^{kj} - (R^{-1})^{km}P^{ml}Q^{lj} \quad . \quad (20)$$

Substituting the expansion coefficients $\alpha^{(q,k)}$ and $\beta^{(q,k)}$ from (20) and (19) into (15), we obtain the approximation of the field variable in terms of the nodal values

$$u(\mathbf{x})|_{\Omega^q} = \sum_{j=1}^{N} u(\mathbf{x}^{n(q,j)})\varphi^{(q,j)}(\mathbf{x}),$$

(21)

in which the shape functions are given as

$$\varphi^{(q,j)}(\mathbf{x}) = \sum_{k=1}^{N} R^{n(q,k)}(\mathbf{x})T^{kj} + \sum_{k=1}^{M} P^k(\mathbf{x})Q^{kj}.$$

(22)

The approximation of potential gradients is given by Eq. (14) with

$$\varphi_{,i}^{(q,j)}(\mathbf{x}) = \sum_{k=1}^{N} R_{,i}^{n(q,k)}(\mathbf{x})T^{kj} + \sum_{k=1}^{M} P_{,i}^k(\mathbf{x})Q^{kj}$$

(23)

and $R_{,i}^{n(q,k)}(\mathbf{x})$, $P_{,i}^k(\mathbf{x})$ being given at the end of the previous subsection.

Let us evaluate the shape function at a local supporting node. According to (22) and the definition (20), we may write, using the brief notation for matrix elements,

$$\varphi^{(q,j)}(\mathbf{x}^{n(q,l)}) = R^{lk}T^{kj} + P^{lk}Q^{kj} =$$

$$R^{lk}\left[(R^{-1})^{kj} - (R^{-1})^{km}P^{ms}Q^{sj}\right] + P^{lk}Q^{kj} = \delta_{lj}.$$

Thus, the shape functions possess the Kronecker delta property.

Note that even P^{jk} is a square matrix provided that $M = N$. Then, in the approach based on the choice of the constraint equation (17), we have

$$(S^{-1})^{lm} = (P^{-1})^{lk}R^{kj}(P^{T-1})^{jm} \quad ,$$

hence $Q^{lj} = (S^{-1})^{lm}(P^T)^{mk}(R^{-1})^{kj} = (P^{-1})^{lj}$ and $T^{kj} = 0$. Thus, the PBF+MQ interpolation approach reduces to simple polynomial basis PBF interpolation with the shape functions

$$\varphi^{(q,j)}(\mathbf{x}) = \sum_{k=1}^{N} P^k(\mathbf{x})\left(P^{-1}\right)^{kj}, \quad j = 1, 2, ..., N \quad . \quad (24)$$

Though the PBF interpolation approach yields good accuracy, the numerical stability of this approach is not guaranteed because of the possible singularity of the matrix P^{jk}.

The other approach based on the use of the Least Square Method (LSM) instead of the constraint equation (17) does not give reasonable numerical results.

4 System of discretized equations

The local integral equations are assumed to be collocated at interior nodal points $\mathbf{x}^c$ with the sub-domain Ω^c being a circle of the radius h and centered at $\mathbf{x}^c$. Then, the discretized LIE is given by

$$\sum_{a=1}^{N} H^{ca} u(\mathbf{x}^{n(c,a)}) = V^c \qquad (25)$$

where

$$V^c = -\int_{\Omega^c} Q(\mathbf{x}) G(\mathbf{x}-\mathbf{y}^c) d\Omega(\mathbf{x})$$

and the H-matrix takes the form

$$H^{ca} = \int_{\partial\Omega^c} \lambda_{ij}(\eta)\varphi_{,j}^{(c,a)}(\eta)n_i(\eta)G(\eta-\mathbf{y}^c)d\Gamma(\eta) -$$

$$\int_{\Omega^c} \lambda_{ij}(\mathbf{x})\varphi_{,j}^{(c,a)}(\mathbf{x})G_{,i}(\mathbf{x}-\mathbf{y}^c)d\Omega(\mathbf{x}) \qquad (26)$$

for the LIE of the 1st kind, and

$$H^{ca} = -\delta_{a1} + \int_{\partial\Omega^c} \left[\lambda_{ij}(\eta)\varphi_{,j}^{(c,a)}(\eta)n_i(\eta)G(\eta-\mathbf{y}^c) -\right.$$

$$\left. \varphi^{(c,a)}(\eta)\lambda_{ij}^c n_j(\eta)G_{,i}(\eta-\mathbf{y}^c)\right]d\Gamma(\eta) -$$

$$\int_{\Omega^c} \tilde{\lambda}_{ij}(\mathbf{x})\varphi_{,j}^{(c,a)}(\mathbf{x})G_{,i}(\mathbf{x}-\mathbf{y}^c)d\Omega(\mathbf{x}) \qquad (27)$$

for the LIE of the 2nd kind.

Now, we need to discretize the boundary conditions. On the Dirichlet part of the boundary, we may write

$$u(\eta^b) = \overline{u}(\eta^b) \text{ at } \eta^b \in \partial\Omega_D,$$

$$\text{since } \sum_{a=1}^{N} u(\mathbf{x}^{n(b,a)})\varphi^{(b,a)}(\eta^b) = u(\eta^b \qquad (28)$$

while on the Neumann part of the boundary, we have

$$n_k(\eta^b)\sum_{a=1}^{N} u(\mathbf{x}^{n(b,a)})\varphi_{,k}^{(b,a)}(\eta^b) = \overline{q}(\eta^b)$$

$$\text{at } \eta^b \in \partial\Omega_N \qquad (29)$$

5 Numerical examples

In order to test the proposed numerical method, we shall consider examples for which analytical solutions are available. The considered domain is either a square $L \times L$ or an angular section of the cross section of a thick-walled tube (see Fig. 3). In the case of square domain, we assume the Dirichlet boundary conditions on both the bottom and top sides

$$\overline{u} = u_o \text{ if } x_2 = 0; \quad \overline{u} = u_L \text{ if } x_2 = L$$

and the Neumann conditions on the lateral sides

$$\overline{q}(\mathbf{x}) = -\lambda_{ij}(\mathbf{x})n_i(\mathbf{x})u_{,j}^{ex}(\mathbf{x}) \text{ if } x_1 = 0 \text{ or } x_1 = L,$$

while the BVP in a thick-walled tube is specified by the Dirichlet boundary conditions on the inner and outer radii

$$\overline{u} = u_a \text{ if } r = a; \ \overline{u} = u_b \text{ if } r = b$$

and the Neumann boundary condition on the radial sections

$$\overline{q} = 0 \text{ if } r \in (a,b) \text{ and } \varphi = 0 \text{ or } \varphi = \alpha.$$

The body source density is vanishing in Ω and the tensor of the material coefficients takes the form $\lambda_{ij}(\mathbf{x}) = L_{ij}\lambda(\mathbf{x})$ with $L_{11} = L_{22} = 2$, $L_{12} = L_{21} = 1$ in anisotropic case, while $L_{ij} = \delta_{ij}$ in isotropic case. The exact solutions will be specified in particular examples according to chosen material coefficients $\lambda_{ij}(\mathbf{x})$. In the case of thick walled-tube only isotropic medium is considered.

In the numerical experiments for the accuracy of the numerical results, we have used the average % error defined as

$$\text{APE}_t = 100\sqrt{\sum_{a=1}^{N_t} [u^c(\mathbf{x}^a) - u^{ex}(\mathbf{x}^a)]^2 / \sum_{a=1}^{N_t} [u^{ex}(\mathbf{x}^a)]^2}, \qquad (30)$$

where N_t is the total number of nodes on closed domain $\Omega \cup \partial\Omega$.

In this paper, we assume the radial basis function shape parameter $m = -2$ and the polynomial basis is given by $n_p = 6$ monomials. The number of the radial basis functions $n_r = n_p$ in the case of *PBF×MQ* interpolation, while $n_r > n_p$ in the case of *PBF+MQ* interpolation.

Example 1

Since the radial basis functions involve the shape parameters m and c, it is interesting to know the influence of such parameters on the accuracy of numerical results obtained by PIM utilizing the radial basis functions.
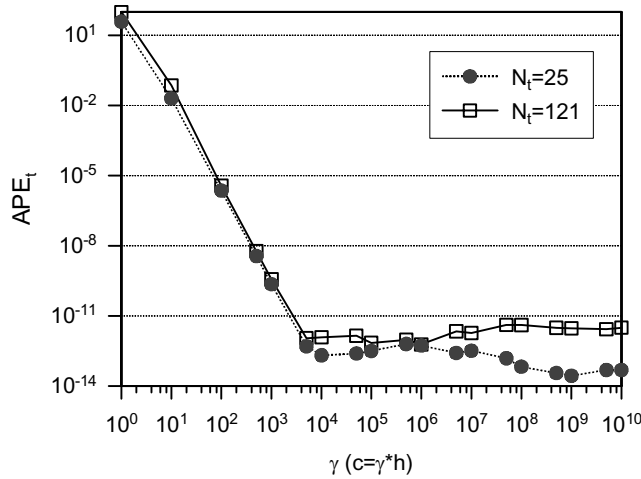

Figure 1 : Influence of the shape factor c on the accuracy of the numerical solution of the considered BVP in a square by using the LIE of the 1st kind and the $PBF \times MQ$ interpolation with $n_r = n_p = 6$

In this example, we investigate the sensitivity of numerical results on the shape parameter $c = \gamma h$, expressed by the dimensionless parameter γ and the characteristic length h defined as the shortest distance of any two nodal points distributed over the closed domain $\Omega \cup \partial\Omega$. We assume homogeneous and isotropic medium. Figures 1 and 2 show the c-sensitivities in the square domain $\Omega = [0, L] \times [0, L]$ with a uniform distribution of nodal points. The characteristic length $h = 0.25L$ when $N_t = 25$ and $h = 0.1L$ when $N_t = 121$.

In the case of the BVP in thick-walled tube, we have considered an angular section of the cross section as shown in Fig. 3 with $\alpha = 4°$ and $a = 10$, $b = 11$. Figures 4 and 5 show the c-sensitivities for $PBF + MQ$ and $PBF \times MQ$, respectively, when uniform distributions of nodal points are used with $N_t = 25$ or 81. Note that the uniform distribution is considered in the sense of uniform distribution in the radial and angular coordinates. The corresponding characteristic lengths are $h = 0.17453$ when $N_t = 25$ and $h = 0.08726$ when $N_t = 81$.
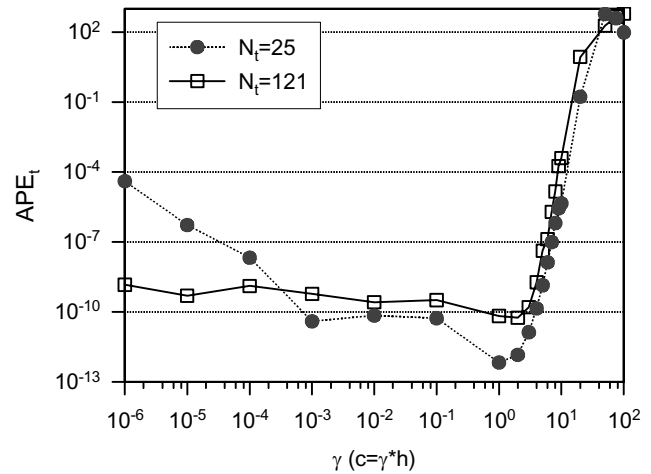

Figure 2 : Influence of the shape factor c on the accuracy of the numerical solution of the considered BVP in a square by using the LIE of the 1st kind and the $PBF + MQ$ interpolation with $n_p = 6$ and $n_r = 16$
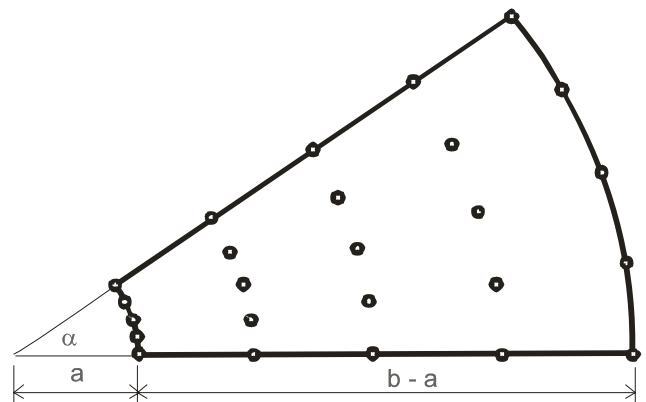

Figure 3 : Angular section of the thick-walled tube cross section with 25 uniformly distributed nodal points

As can be seen from both the analyzed examples, the c-sensitivity is inexpressive and accuracy acceptable for $\gamma \geq 10^4$ in the case of $PBF \times MQ$ interpolation, while for $\gamma \leq 1$ in the case of $PBF + MQ$ interpolation.

Example 2

In this example, we study the stability of numerical results with respect to the distribution of nodal points. Three different meshfree interpolations are applied to the considered BVP in the square domain. Six polynomial basis functions ($n_p = 6$) are employed for in-
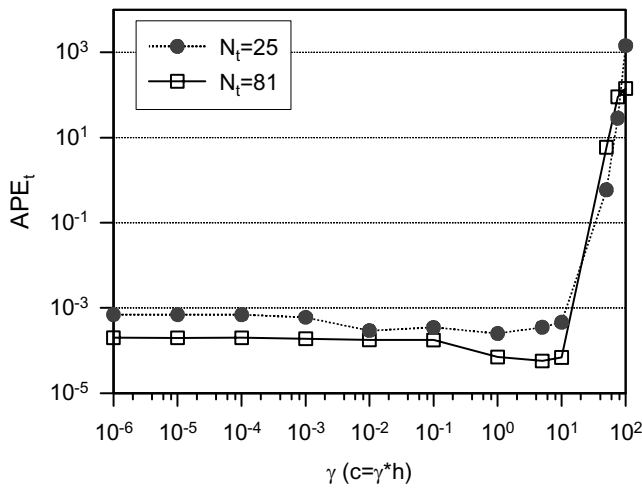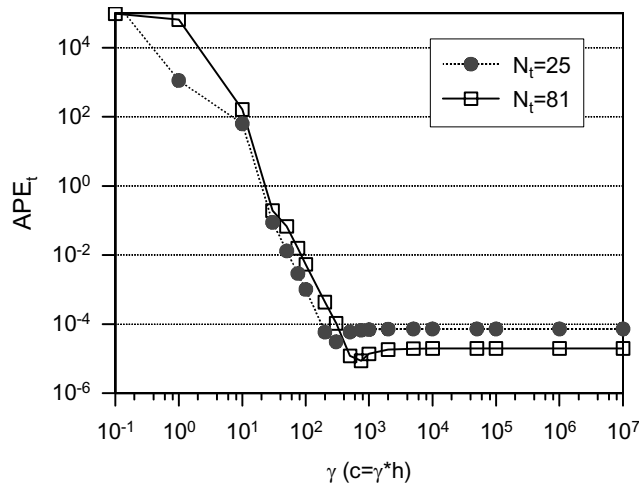
Figure 4 : Influence of the shape factor c on the accuracy of the numerical solution of the considered BVP in the thick-walled tube by using the LIE of the 1st kind and the $PBF + MQ$ interpolation with n_p=6 and n_r=10

Fig. 6.

Figure 6 : Distributions of nodal points in a square domain

Figure 5 : Influence of the shape factor c on the accuracy of the numerical solution of the considered BVP in the thick-walled tube by using the LIE of the 1st kind and the $PBF \times MQ$ interpolation with $n_r = n_p$=6

terpolation at any point by using each of the interpolations ($PBF, PBF \times MQ, PBF + MQ$). The number of the radial basis functions n_r is equal to n_p if $PBF \times MQ$ interpolation is used, while in the case of $PBF + MQ$ interpolation it is variable with $n_r > n_p$. For illustration, we present the numerical results for four different distributions of nodal points denoted as $DNP(i)$ and shown in

Recall that $DNP(1)$ is a uniform distribution, while the rest ones are non-uniform with the total numbers of nodes $N_t = 25, 25, 16, 19$, respectively.

As can be seen from Fig. 7, the accuracies of the numerical solution of the BVP in a square domain by the PBF and/or $PBF \times MQ$ interpolations are not stable with respect to variations of the nodal points distribution. On the other hand, an acceptable accuracy is achieved by $PBF + MQ$ interpolation for each distribution of nodal points when a sufficient number of radial basis functions is employed.

The instability of the accuracy by using the PBF and/or $PBF \times MQ$ interpolations can be confirmed also by failure of the patch tests when non-uniform distributions of nodal points are utilized. Fig.8 shows the maximal relative error of the approximated field $u(x_1, x_2) = x_1 x_2$ over the square $[1, 2] \times [1, 2]$ when four different distributions of nodal points are used. Strictly speaking

$$\text{max error} = \max_{x_1, x_2} \left\{ \left| \frac{u^{appr} - x_1 x_2}{x_1 x_2} \right| \right\}, \quad x_1, x_2 \in [1, 2].$$
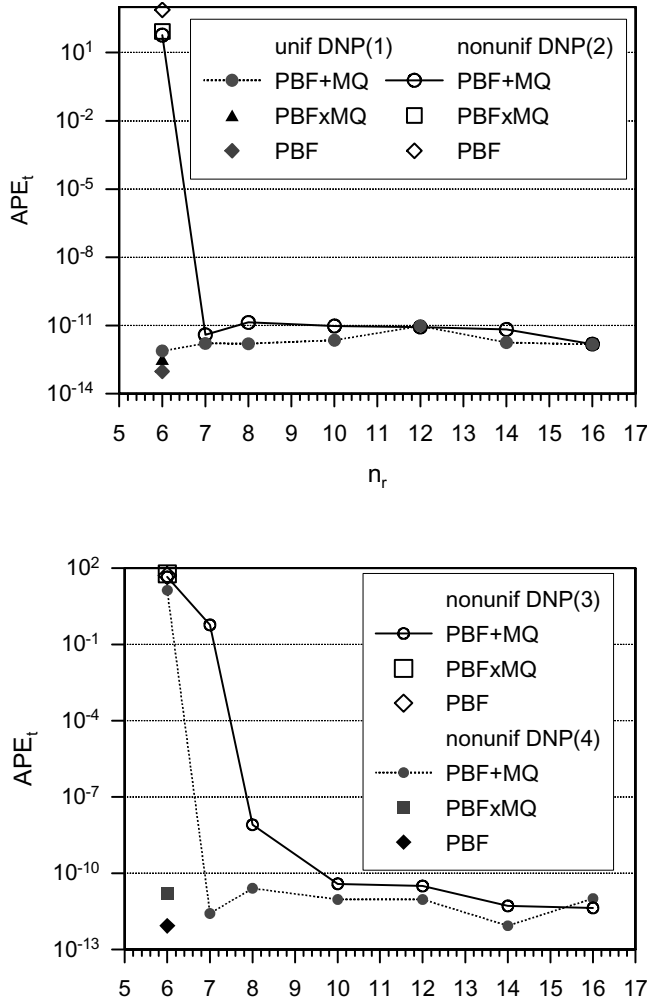
Figure 7 : Accuracies of numerical results obtained by using three different meshless interpolation approaches and four different distributions of nodal points. Dependence of the accuracy by $PBF + MQ$ on the number of employed radial basis functions

Example 3

In this example, we study the accuracy of numerical solutions of the BVP in a square domain filled with a homogeneous medium $\lambda(\mathbf{x}) = const$ by using various implementations of the LIE. Then, the analytical solution is given as

$$u^{ex}(\mathbf{x}) = u_o + (u_L - u_o)x_2/L,$$

$$q_i^{ex}(\mathbf{x}) = -L_{i2}(u_L - u_o)/L. \tag{31}$$

Note that the flux on the lateral sides of the square domain (Neumann parts of the boundary) vanishes only in
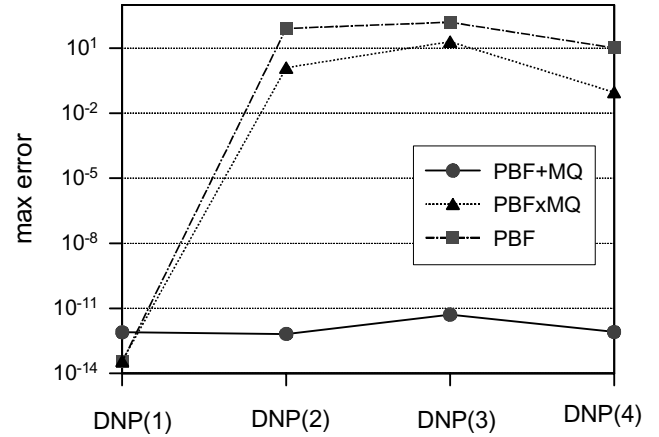
Figure 8 : Maximal errors for patch tests in a square achieved by *PBF, PBFxMQ, PBF+MQ* interpolations with $n_p=6$ and further specifications as: $\gamma = 10^7$ for $PBF \times MQ$; $\gamma = 2$ and $n_r=10$ for $PBF+MQ$

the case of an isotropic medium. Fig. 9 is a comparison of accuracies by three meshfree interpolations as well as by using the mesh of quadrilateral elements with quadratic approximation [Sladek et al (2004)]. The accuracy in each numerical solution is evaluated by Eq. (30) with using the exact solution as a benchmark solution. Only the uniform distribution of nodal points is employed with using h/L as a dimensionless parameter for characterization of the density of the nodal point distribution. The meshfree interpolations are specified as: $n_p = 6$; $n_r = n_p$ and $\gamma = 10^7$ in the case of $PBF \times MQ$ interpolation, while $n_r = 16$ and $\gamma = 2$ in the case of $PBF + MQ$ interpolation.

The increase of the nodal point density and/or the order of the interpolation can improve the approximation of both the geometrical and field variables in some problems. On the other hand, the increase of the number of nodal points (nodal unknowns) gives rise to calculation errors. In the analyzed simple problem in homogeneous medium, the exact solution is linear dependent on the x_2-coordinate. The integration along straight lines is exact and the domain integrals are not involved. Thus, no improvement of the accuracy is expected with increasing the number of nodal points as compared with the accuracy achieved by using the coarsest distribution of nodal points. This expectation is confirmed in Fig. 9.
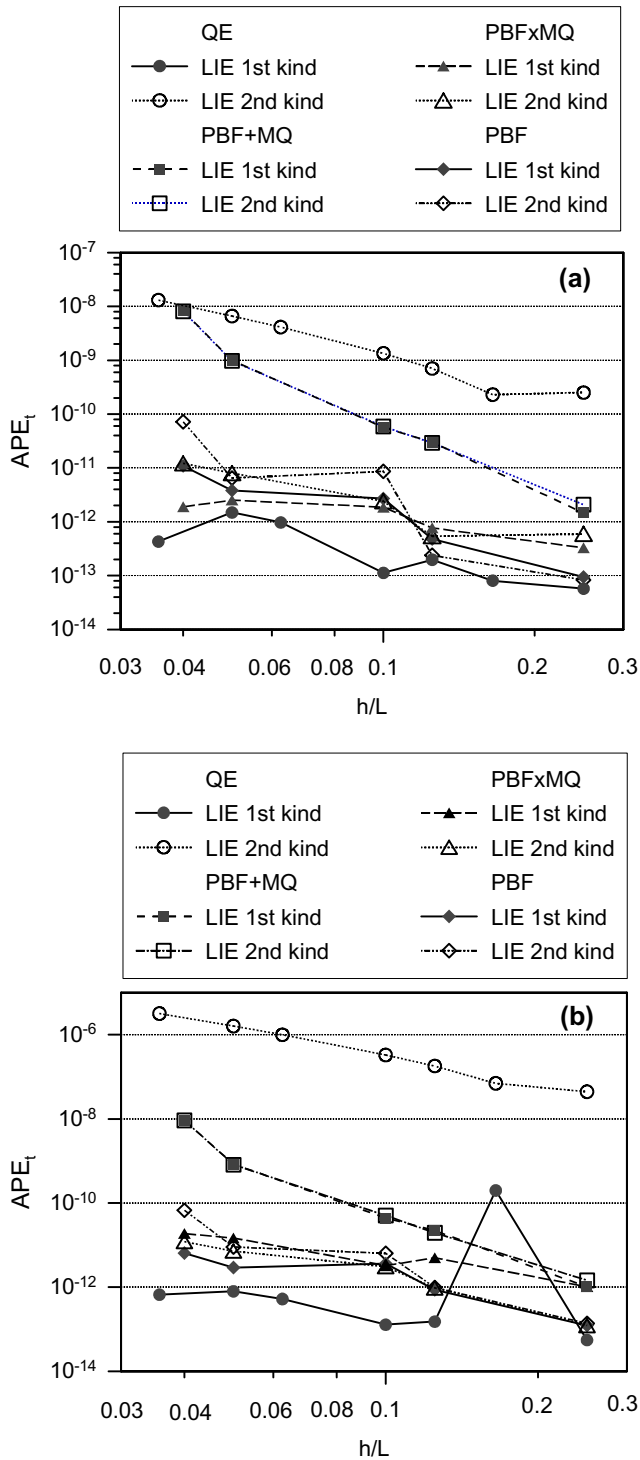
It is interesting to compare the CPU-times consumed in

numerical solutions by particular interpolation schemes. Fig. 10 corresponds to solution of the BVP in homogeneous anisotropic medium but the CPU-times are changed only negligibly in the case of isotropic medium.
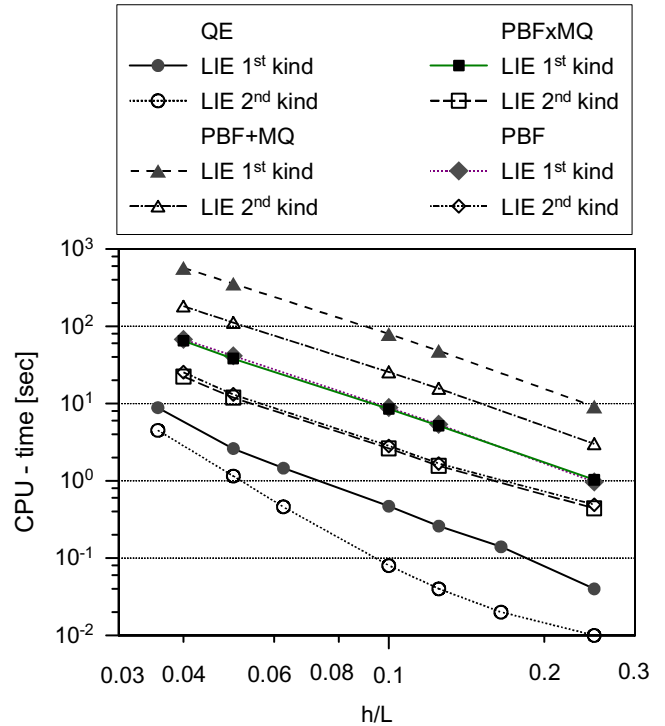

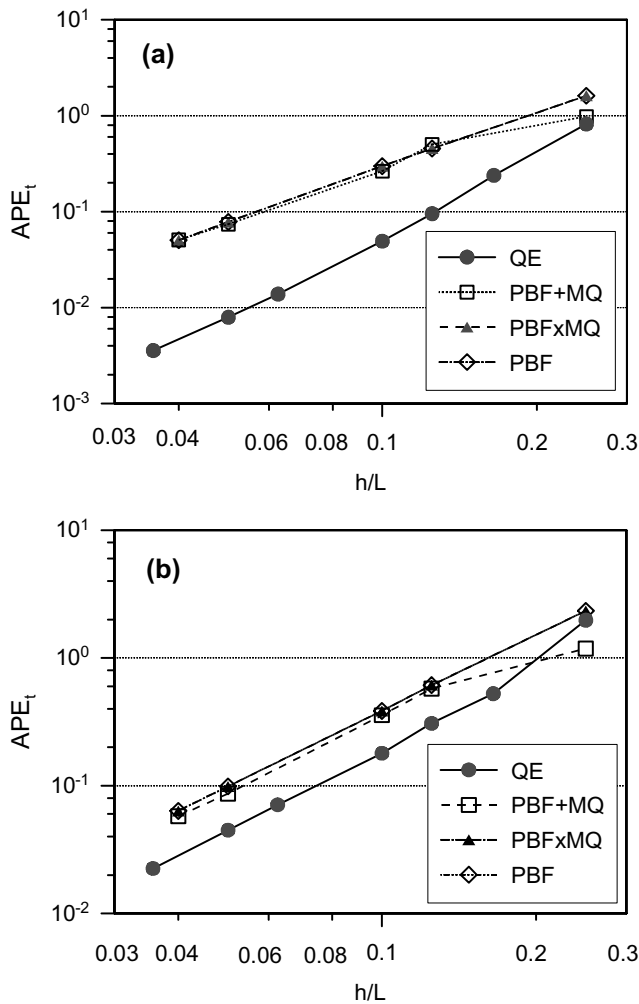**Figure 10** : Dependence of CPU-times on the density of nodal point distribution

Figure 9 : Dependence of accuracy on the density of the distribution of nodal points in: (a) isotropic; (b) anisotropic homogeneous medium

It can be seen that the meshfree interpolation schemes require approximately by one order longer CPU-time than the standard discretization approach utilizing quadrilateral mesh. Moreover, the use of $PBF + MQ$ interpolation with $n_r = 16$ needs another enhancement of the CPU-time by one order. On the other hand, the CPU-times corresponding to the approaches based on the LIE of the 2nd kind take approximately one third of the CPU-times corresponding to the LIE of the 1st kind. This is so because the former approach does not involve any integration over subdomains. In the case of nonhomogeneous media, the domain integration is required in each approach and the CPU-times are almost independent on the material properties. Thus, the CPU-times for the LIE of the 1st kind shown in Fig. 10 represent also the CPU-times using either the LIE of the 1st or 2nd kind in non-

homogeneous, isotropic and/or anisotropic media.

Example 4

Now, we consider a non-homogeneous medium with exponentially graded material coefficients described by $\lambda(\mathbf{x}) = e^{\delta x_2/L}$. Then, the analytical solution in the square domain is given as

$$u^{ex}(\mathbf{x}) = u_o + (u_L - u_o)(1 - e^{-\delta x_2/L})/(1 - e^{-\delta}),$$
$$q_i^{ex}(\mathbf{x}) = -L_{i2}(u_L - u_o)\delta/(1 - e^{-\delta})L. \qquad (32)$$

(a)

(b)

Figure 11 : Dependence of accuracy on the density of the distribution of nodal points in: (a) isotropic (b) anisotropic non-homogeneous medium with exponential gradation

In contrast to the previous example, the accuracy is now improved with increasing the density of nodal point dis-

tribution. The error due to the numerical treatment of the domain integral contribution of the non-homogeneity term is dominant and the accuracy by the LIE of the 1st kind is the same as that by the LIE of the 2nd kind.

As can be seen, the convergence rate with increasing the nodal point distribution density is almost the same for any of the studied interpolation.

Example 5

In order to test the proposed computational techniques also for another kind of continuous non-homogeneity, let us consider the same BVP as in the previous example but with a power-law gradation of the material coefficient.

Assuming the quadratic variation of the material coefficient given by $\lambda(\mathbf{x}) = (1 + \delta x_2/L)^2$, we may write the analytical solution as

$$u^{ex}(\mathbf{x}) = u_o + (u_L - u_o)\frac{(1 + \delta x_2/L)^{-1} - 1}{(1 + \delta)^{-1} - 1},$$
$$q_i^{ex}(\mathbf{x}) = L_{i2}\frac{\delta}{L}\frac{u_L - u_o}{(1 + \delta)^{-1} - 1} . \qquad (33)$$

The Dirichlet boundary conditions on the bottom and the top of the square have been specified as $u_o = 1$ and $u_L = 20$. Te results of the convergence study are shown in Fig. 12.

Example 6

Finally, in this example we apply all the considered interpolation approaches to solution of the Dirichlet BVP in a thick-walled tube. The BVP is considered in a narrow angular section of the cross section of the tube as shown in Fig. 3. The material medium is isotropic either homogeneous or continuously nonhomogeneous with exponential and/or power-law gradation of the material coefficient in the radial direction. The analytical solution is given [Sladek et al (2004)]:

(i) for homogeneous material medium $\lambda_{ij}(\mathbf{x}) = \delta_{ij}\lambda_o$ as

$$u(r) = u(a) + \frac{u(b) - u(a)}{\ln b - \ln a}[\ln r - \ln a] \quad , \qquad (34)$$

(ii) for exponentially graded material coefficient

$$\lambda_{ij}(\mathbf{x}) = \delta_{ij}\lambda_o e^{\delta(r-a)/(b-a)} \text{ as}$$

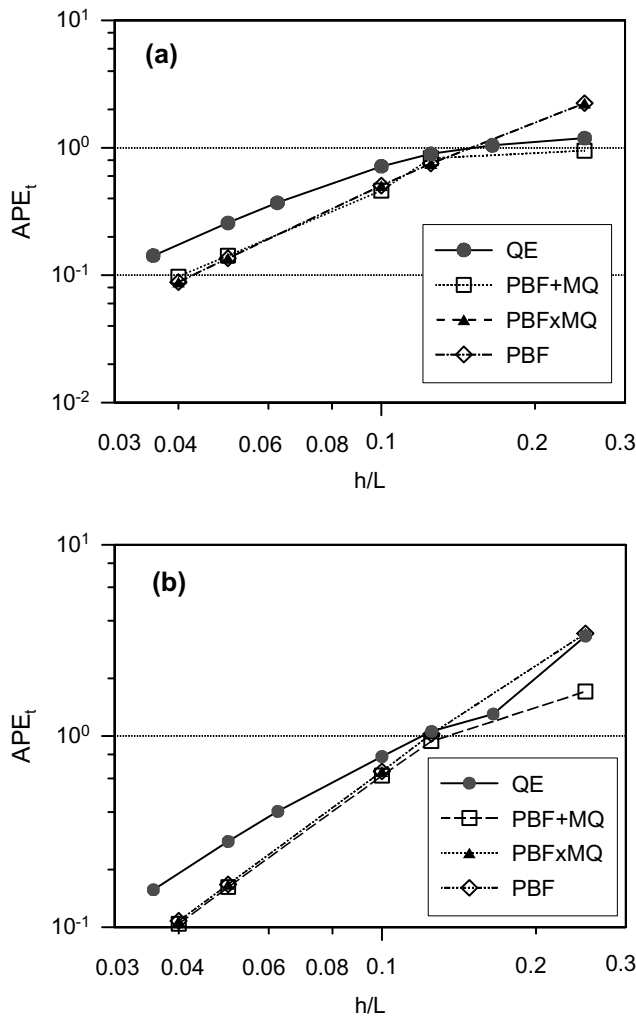$$u(r) = u(a) + \frac{u(b) - u(a)}{E_1(\gamma b) - E_1(\gamma a)}[E_1(\gamma r) - E_1(\gamma a)], \quad (35)$$

Figure 12 : Dependence of accuracy on the density of the distribution of nodal points in: (a) isotropic (b) anisotropic non-homogeneous medium with power-law gradation

where $E_1(z)$ is the Exponential integral function [Abramowitz and Stegun (1964)],

(iii) for the power-law graded material coefficient

$\lambda(r) = \left(1 + \delta\frac{r-a}{b-a}\right)^n$ with $n = 2$ as

$$u(r) = u(a) + \frac{u(b) - u(a)}{I(b) - I(a)}[I(r) - I(a)],\qquad(36)$$

where $I(r)$ is expressed in terms of elementary functions by

$$I(r) = \frac{1}{A^2}\left[\frac{A}{A + \gamma r} + \ln\frac{r}{A + \gamma r}\right],$$

$$A = 1 - \gamma a,\ \gamma = \frac{\delta}{b - a}\quad.$$

For the numerical evaluation of the Exponential integral function, one can use its continued fraction representation together with the modified Lentz's algorithm [Press et al (1988)].

Fig. 13 shows the accuracy of numerical solutions of the considered BVP in the tubes of various material properties. In the case of nonhomogeneous media, there is no difference between the results by the LIE of the 1st and 2nd kinds. Convergence of the numerical results to the exact ones can be observed in nonhomogeneous media and partially also in solutions for the homogeneous medium.
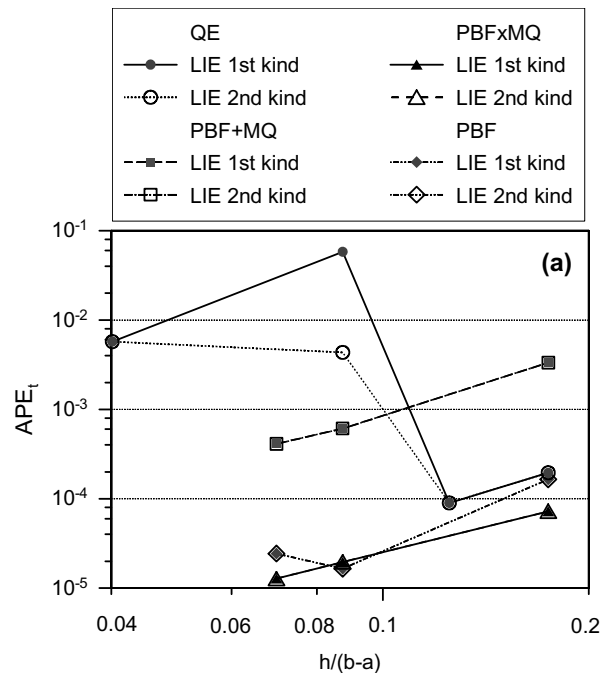

Figure 13a : The dependence of accuracy on the density of the distribution of nodal points in homogeneous medium

Finally, note that the CPU-times shown in Fig. 14 exhibit the same character as in the case of square domain

6   Conclusions

A new numerical method is developed for the solution of 2-d potential problems in anisotropic and continuously non-homogeneous media. The method is based on the
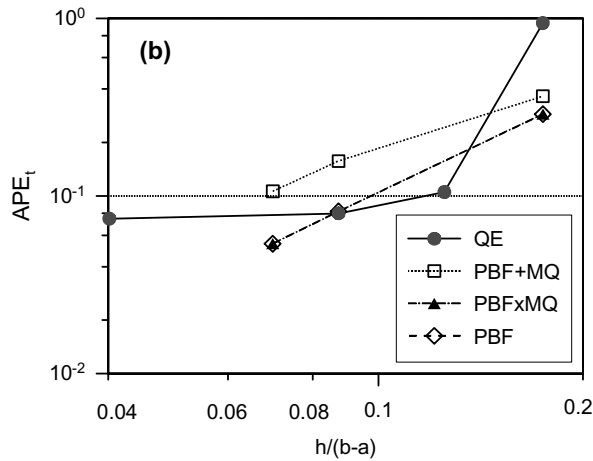
Figure 13b : The dependence of accuracy on the density of the distribution of nodal points in non-homogeneous medium with exponentially graded material coefficient and the grade parameter $\delta = 3$
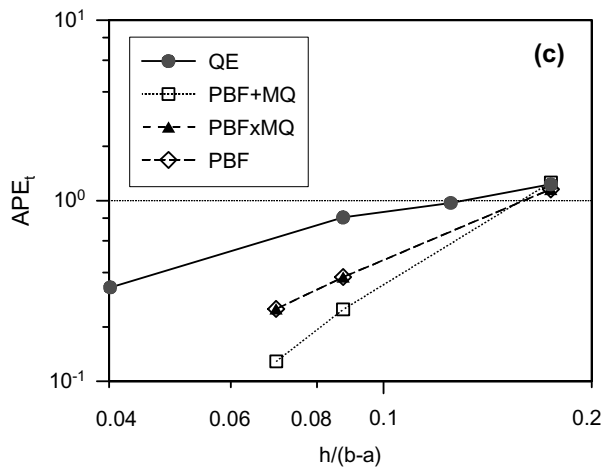

Figure 13c : The dependence of accuracy on the density of the distribution of nodal points in c) nonhomogeneous medium with power-law graded material coefficient and the grade parameter $\delta = 3$

local integral equations and meshfree approximations by using three different point interpolation methods. The integral equations are nonsingular and the shape functions of the applied interpolations possess the Kronecker-delta property.

The use of the polynomial basis functions combined with radial basis multiquadrics exhibits sensitivity of the accuracy of numerical results on the shape parameter c in-
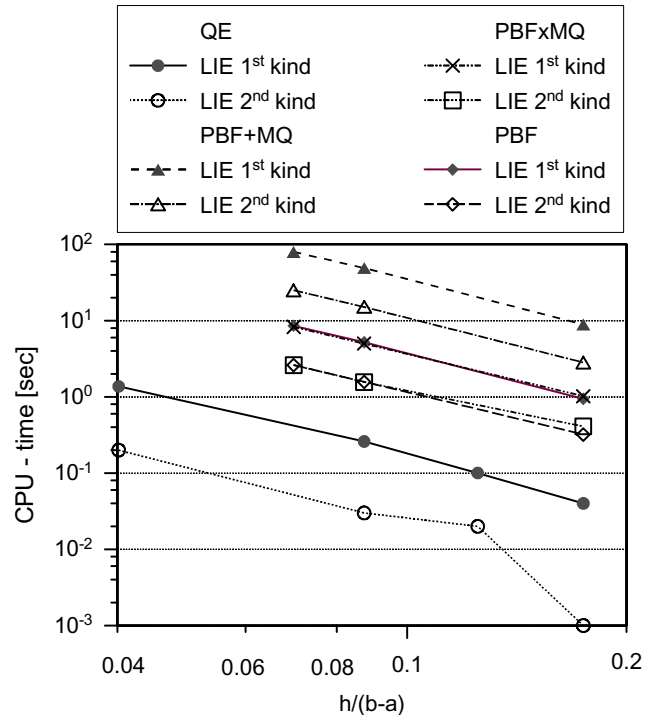

Figure 14 : Dependence of CPU-times on the density of nodal point distribution in homogeneous tube

volved in the multiquadrics. Nevertheless, in both the combinations $PBF \times MQ$ and $PBF + MQ$ one can specify a wide range of c-values on which the accuracy is rather insensitive.

The study of the stability of numerical results as well as patch tests on the distribution of nodal points within the sample indicates the instability when using PBF and/or $PBF \times MQ$ interpolations with non-uniform distributions of nodal points. On the other hand, the $PBF + MQ$ interpolation with sufficient amount of radial basis functions yields stable numerical results.

As regards the accuracy achieved by the LIE of the 1st and 2nd kinds, there is a difference only in the case of the BVP in a square domain of homogeneous media. Remarkably shorter CPU-times are consumed with using the LIE of the 2nd kind in homogeneous media because of the absence of domain integrations. In the case of non-homogeneous media, the domain integration is required in both the approaches and the CPU-times are almost independent on the material properties. The domain integral seems to be dominant also for determination of the accuracy in nonhomogeneous media, since various

meshfree interpolations result in almost the same accuracy. The convergence rate with increasing the density of nodal points distribution in meshfree interpolations is very close to that achieved by using standard domain discretization with using quadrilateral quadratic serendipity elements.

Despite of the instability, the accuracy obtained in numerical solution of the considered BVPs by either the PBF or $PBF \times MQ$ interpolation appears to be very reasonable when uniform distribution of nodal points is employed. The stability of numerical results by the $PBF + MQ$ interpolation is achieved in price of a remarkable increase of the CPU-time. Finally, the CPU-times consumed by the meshfree interpolations are substantially longer than those by using the domain discretization approach.

The proposed method is quite general and a satisfactory accuracy is achieved in our numerical tests. The system matrix is sparse like in the finite element method and the solution is fast.

The method is open for the use of other meshfree approximations. The extension of the method to three dimensions as well as to other applications is straightforward.

References

Abramowitz, M.; Stegun, I. A. (1964): *Handbook of Mathematical Functions, Applied Mathematics Series*. Dover Publications, New York, 1046 pages.

Atluri, S. N.; Zhu, T. (1998a): A new meshless local Petrov-Galerkin (MLPG) approach to nonlinear problems in computational modeling and simulation. *Comput. Modeling Simulation in Engrg*., vol. 3, pp. 187-196.

Atluri, S. N.; Zhu, T. (1998b): A new meshless local Petrov-Galerkin (MLPG) approach in computational mechanics. *Comput. Mech.*, vol. 22, pp. 117-127.

Atluri, S. N.; Zhu, T. (1999): The meshless local Petrov-Galerkin (MLPG) approach for solving problems in elasto-statics. *Comput. Mech.*, vol. 25, pp. 169-179.

Atluri, S. N.; Shen, S. (2002a): *The Meshless Local Petrov-Galerkin (MLPG) Method*. Tech Science Press, Encino, 429 pages.

Atluri, S. N.; Shen, S. (2002b): The meshless local Petrov-Galerkin (MLPG) method: A simple & less-costly alternative to the finite element and boundary element method. *CMES: Computer Modeling in Engineering & Sciences*, vol. 3, pp. 11-52.

Atluri, S. N. (2004): *The Meshless Method (MLPG) for Domain & BIE Discretizations*, Tech Science Press, Forsyth, GA, 688 pages.

Chang, Y. P.; Kang, C. S.; Chen, D. J. (1973): The use of fundamental Green's functions for the solution of problems of heat conduction in anisotropic media. *Jour. Heat Mass Transf.*, vol. 16, pp. 1905-1918.

Golberg, M. A.; Chen, C. S.; Bowman, H. (1999): Some recent results and proposals for the use of radial basis functions in the BEM. *Engn. Anal. Bound. Elem.*, vol. 23, pp. 285-296.

Hardy, R. L. (1990): Theory and applications of the multiquadrics-biharmonic method (20 years of discovery 1968-1988). *Comput. Math. Appl.*, vol. 19, pp. 163-208.

Li, Q.; Shen, S.; Han, Z. D.; Atluri, S. N. (2003): Application of meshless local Petrov-Galerkin (MLPG) to problems with singularities, and material discontinuities, in 3-D elasticity. *CMES: Computer Modeling in Engineering & Sciences*, vol. 4, pp. 571-585.

Liu, G. R. (2003): *Mesh Free Methods, Moving beyond the Finite Element Method*. CRC Press, Boca Raton, 691 pages.

Mikhailov, S. E. (2002): Localized boundary-domain integral formulations for problems with variable coefficients. *Eng. Anal. Bound. Elem.*, vol. 26, pp. 681-690.

Mikhailov, S. E.; Nakhova, I. S. (2003): Numerical solution of a Neumann problem with variable coefficients by the localized boundary-domain integral equation method. In: Sia Amini (ed) *Fourth UK Conf. on Boundary Integral Methods*, Salford University, UK, ISBN 0-902896-40-7, pp. 175-184.

Miyamoto, Y.; Kaysser, W. A.; Rabin, B. H., Kawasaki, A.; Ford, R. G. (1999): *Functionally Graded Materials, Design, Processing and Applications*. Kluwer Academic Publishers, Dordrecht, 330 pages.

Press, W. H.; Teukolsky, S. A.; Vetterling, W. T.; Flannery, B. P. (1988-1992): *Numerical Recipes in C:*

The Art of Scientific Computing. Cambridge University Press, 1032 pages.

Sladek, J.; Sladek, V.; Atluri, S. N. (2002): Application of local boundary integral equation method to solve boundary value problems. *Int. J. Appl. Mech.*, vol. 38, pp. 3-27.

Sladek, J.; Sladek, V.; Atluri, S. N. (2004a): Meshless local Petrov-Galerkin method for heat conduction problem in an anisotropic medium. *CMES: Computer Modeling in Engineering & Sciences*, vol. 6, pp. 309-318.

Sladek, J.; Sladek, V.; Atluri, S. N. (2004b): Meshless local Petrov-Galerkin method in anisotropic elasticity. *CMES: Computer Modeling in Engineering & Sciences*, vol. 5, pp. 477-489.

Sladek, V.; Sladek, J. (2000): Global & local integral equations for potential problems in non-homogeneous media. *CTU Report*, vol. 4, pp. 133-138.

Sladek, V.; Sladek, J.; Van Keer, R. (2002): New integral equation approach to solution of diffusion equation. *Comp. Assist. Mech. Engn. Sci.*, vol. 9, pp. 555-572.

Sladek, V.; Sladek, J. (2003): A new formulation for solution of boundary value problems using domain-type approximations and local integral equations. *Electronic Jour. Bound. Elem.*, vol. 1, pp. 132-153.

Sladek, V.; Sladek, J.; Zhang, Ch. (2004): Local integro-differential equations with domain elements for numerical solution of PDE with variable coefficients. *Jour. Eng. Mathematics*, in print.

Wrobel, L.C. (2002): *The Boundary Element Method, Vol. 1: Applications in Thermo-Fluids and Acoustics*. John Wiley & Sons Ltd., Chichester, England, 451 pages.

Zhu, T.; Zhang, J. D.; Atluri, S. N. (1998): A local boundary integral equation (LBIE) method in computational mechanics, and a meshless discretization approach. *Comput. Mech.*, vol. 21, pp. 223-235.